

Phenomenological implications of two simple modifications to Tri-Bimaximal mixing

Kanwaljeet S. Channey

*Department of Physics and Astrophysics, University of Delhi,
Delhi, 110007, India.*

kjschanney@outlook.com

Sanjeev Kumar

*Department of Physics and Astrophysics, University of Delhi,
Delhi, 110007, India.*

sanjeevkumarverma@outlook.in

We study the phenomenological implications of breaking the Tri-Bimaximal (TBM) mixing in such a way that either first or second column of TBM mixing matrix remains invariant. We present two such textures and confront them with the experimental data. We give the predictions of these textures for atmospheric mixing angle θ_{23} and Dirac-type CP violating phase δ that will be measured in the future experiments.

One of the unresolved mysteries of the neutrino physics is the origin of the neutrino masses. If the three neutrino masses are distinct and non zero, the mass and flavour eigen states of neutrinos are not identical. The flavour eigen states (ν_f) can be written as a linear combination of the mass eigen states (ν_i):

$$\nu_f = U \nu_i. \quad (1)$$

Here, $i = 1, 2, 3$ and $f = e, \mu, \tau$. The neutrino mixing matrix, U , is given as¹

$$U = \begin{pmatrix} c_{12}c_{13} & s_{12}c_{13} & s_{13}e^{-i\delta} \\ -s_{12}c_{23} - c_{12}s_{23}s_{13}e^{i\delta} & c_{12}c_{23} - s_{12}s_{23}s_{13}e^{i\delta} & s_{23}c_{13} \\ s_{12}s_{23} - c_{12}c_{23}s_{13}e^{i\delta} & -c_{12}s_{23} - s_{12}c_{23}s_{13}e^{i\delta} & c_{23}c_{13} \end{pmatrix}, \quad (2)$$

where $s_{ij} = \sin \theta_{ij}$ and $c_{ij} = \cos \theta_{ij}$ for $i, j = 1, 2, 3$ and θ_{12} , θ_{23} , θ_{13} are the three mixing angles. The phase δ is responsible for Dirac-type CP violation in neutrino oscillations. The mixing matrix (U) diagonalizes the neutrino mass matrix (M_ν) as

$$U^T M_\nu U = M_\nu^{\text{diag}} \quad (3)$$

where, the diagonal neutrino mass matrix is $M_\nu^{\text{diag}} = \text{diag}\{m_1, m_2 e^{2i\alpha}, m_3 e^{2i\beta}\}$. Here, the phases α and β are the Majorana phases. These phases do not appear in the oscillation probabilities. However, they can be constrained in the neutrino

less double beta decay experiments. If the three neutrino masses (m_1, m_2 and m_3), three neutrino mixing angles (θ_{12}, θ_{23} and θ_{13}) and the three CP violating phases (α, β, δ) are known, the neutrino mass matrix can be reconstructed as

$$M_\nu = U^* M_\nu^{\text{diag}} U^\dagger. \quad (4)$$

The reconstruction of the neutrino mass matrix results into many possible structures. The experimental measurements of a non-zero θ_{13} ^{2–5} ruled out many such structures. One such structure corresponded to the Tri-BiMaximal (TBM) mixing⁶ that predicts $\theta_{13} = 0$ and $\theta_{23} = \frac{\pi}{4}$. After the measurement of non-zero θ_{13} , the TBM scheme cannot be compatible with the neutrino data at the leading order. Yet, one can modify the mass matrix corresponding to the TBM mixing (M_{TBM}) by adding some correction terms that break the underlying symmetry of M_{TBM} . However, such modifications need not break the symmetry of M_{TBM} completely. We can modify M_{TBM} in such a manner that the resulting mixing matrix still has its first or second column identical to the TBM mixing matrix U_{TBM} . Such mixing schemes can be called Tri-Maximal (TM) mixing of first and second kind (TM₁^{7–12} and TM₂^{7,9–17}), respectively.

In the present work, we propose two simple textures that can modify M_{TBM} to have non-zero θ_{13} and non-maximal θ_{23} while preserving its first or second eigen vector at its TBM value. We study the phenomenology of these textures and confront them with the experimental data. Our textures are testable at the future neutrino experiments like NO ν A¹⁸ and T2K² that aim to measure the octant of θ_{23} and CP violating phase δ . We also present the predictions of these textures for the Majorana phases (α and β) and the neutrino masses as measured in beta decay,¹⁹ neutrino less double beta decay²⁰ and cosmological experiments.²¹

The TBM mass matrix can be written as

$$M_{\text{TBM}} = \begin{pmatrix} a & c & c \\ c & a+b & c-b \\ c & c-b & a+b \end{pmatrix}. \quad (5)$$

It can be diagonalized as

$$U_{\text{TBM}}^T M_{\text{TBM}} U_{\text{TBM}} = M_\nu^{\text{diag}} \quad (6)$$

where

$$U_{\text{TBM}} = \begin{pmatrix} \sqrt{\frac{2}{3}} & \sqrt{\frac{1}{3}} & 0 \\ -\sqrt{\frac{1}{6}} & \sqrt{\frac{1}{3}} & \sqrt{\frac{1}{2}} \\ -\sqrt{\frac{1}{6}} & \sqrt{\frac{1}{3}} & -\sqrt{\frac{1}{2}} \end{pmatrix}. \quad (7)$$

The neutrino mass matrices for the mixing schemes TM₁^{7–12} and TM₂^{7,9–17} can be written as

$$M_{\text{TM}_i} = M_{\text{TBM}} + M'_{\text{TM}_i} \quad (8)$$

where $i = 1, 2$ corresponds to TM_1 and TM_2 mixings. The general forms of these modified mass matrices can be written as

$$M_{\text{TM}_1} = \begin{pmatrix} a & 2c-d & d \\ 2c-d & a+b+4(c-d) & -b-c+2d \\ d & -b-c+2d & a+b \end{pmatrix} \quad (9)$$

and

$$M_{\text{TM}_2} = \begin{pmatrix} a & c & d \\ c & a+b-c+d & c-b \\ d & c-b & a+b \end{pmatrix}. \quad (10)$$

The most general form of M'_{TM_i} will be similar to M_{TM_i} . However, we do not work with the most general forms as they have too many free parameters. We assume simple textures of M_{TBM} and M'_{TM_i} that are compatible with the neutrino data. The two textures studied in this work are

$$M_i = M_0 + M'_i \quad (11)$$

where $M_i = M_{\text{TM}_i}$ with $c = a$ and $d = a + \mu$ for $i = 1, 2$. Here, the parameter a , b , and c are real while $\mu = ze^{i\chi}$ is a complex parameter. Therefore, our textures have four real parameters *i.e.* a , b , z , and χ . The textures for M_0 and M'_i are

$$M_0 = \begin{pmatrix} a & a & a \\ a & a+b & a-b \\ a & a-b & a+b \end{pmatrix}, M'_1 = \begin{pmatrix} 0 & -\mu & \mu \\ -\mu & -4\mu & 2\mu \\ \mu & 2\mu & 0 \end{pmatrix}, M'_2 = \begin{pmatrix} 0 & 0 & \mu \\ 0 & \mu & 0 \\ \mu & 0 & 0 \end{pmatrix}. \quad (12)$$

The assumption $c = a$ leads to a vanishing lowest mass eigenvalue of M_0 . The modification term M'_i may modify the eigenvalues of M_0 and we may end up with a non-zero value of m_1 . The parameter z acts as the modification parameter and gives us a non-zero θ_{13} and non-maximal θ_{23} . The resulting textures M_i will have normal hierarchy. However, we could construct similar textures for inverted hierarchy by setting $c = a + 2b$ and $d = a + \mu$ in Eqs. (9-10).

The mass matrices M_i can be diagonalized using the relation

$$M_i^{\text{diag}} = U_{\text{TM}_i}^T M_i U_{\text{TM}_i} \quad (13)$$

where

$$U_{\text{TM}_1} = \begin{pmatrix} \sqrt{\frac{2}{3}} & \frac{\cos \theta}{\sqrt{3}} & \frac{\sin \theta}{\sqrt{3}} \\ -\frac{1}{\sqrt{6}} & \frac{\sqrt{\frac{2}{3}} \cos \theta - e^{i\phi} \sin \theta}{\sqrt{2}} & \frac{e^{i\phi} \cos \theta + \sqrt{\frac{2}{3}} \sin \theta}{\sqrt{2}} \\ -\frac{1}{\sqrt{6}} & \frac{\sqrt{\frac{2}{3}} \cos \theta + e^{i\phi} \sin \theta}{\sqrt{2}} & \frac{\sqrt{\frac{2}{3}} \sin \theta - e^{i\phi} \cos \theta}{\sqrt{2}} \end{pmatrix} \quad (14)$$

4

and

$$U_{\text{TM}_2} = \begin{pmatrix} \sqrt{\frac{2}{3}} \cos \theta & \frac{1}{\sqrt{3}} & \sqrt{\frac{2}{3}} \sin \theta \\ \frac{e^{i\phi} \sin \theta - \frac{\cos \theta}{\sqrt{3}}}{\sqrt{2}} & \frac{1}{\sqrt{3}} & \frac{-e^{i\phi} \cos \theta - \frac{\sin \theta}{\sqrt{3}}}{\sqrt{2}} \\ -\frac{\frac{\cos \theta}{\sqrt{3}} - e^{i\phi} \sin \theta}{\sqrt{2}} & \frac{1}{\sqrt{3}} & \frac{e^{i\phi} \cos \theta - \frac{\sin \theta}{\sqrt{3}}}{\sqrt{2}} \end{pmatrix}. \quad (15)$$

Here, θ and ϕ are the two free parameters of the TM_1 and TM_2 mixing matrices. The experimental values of the three mixing angles and the Jarlskog rephasing invariant measure of CP violation J^{22} can be calculated in terms of θ and ϕ using the relations

$$\sin^2 \theta_{12} = \frac{|(U_i)_{12}|^2}{1 - |(U_i)_{13}|^2}, \quad (16)$$

$$\sin^2 \theta_{23} = \frac{|(U_i)_{23}|^2}{1 - |(U_i)_{13}|^2}, \quad (17)$$

$$\sin^2_{13} = |(U_i)_{13}|^2, \quad (18)$$

and

$$J = \text{Im}[(U_i)_{11}(U_i)_{12}^*(U_i)_{21}^*(U_i)_{22}]. \quad (19)$$

We calculate the M_i^{diag} for the textures M_1 and M_2 using Eq. (13). We find that the off-diagonal elements $(M_1^{\text{diag}})_{12}$, $(M_1^{\text{diag}})_{13}$, $(M_2^{\text{diag}})_{12}$ and $(M_2^{\text{diag}})_{23}$ are zero identically. The remaining off-diagonal elements, $(M_1^{\text{diag}})_{23}$ and $(M_2^{\text{diag}})_{13}$, are in general functions of θ and ϕ . Equating them to zero, we obtain the predictions of our textures for θ and ϕ in terms of the four free parameters a , b , z , and χ . Solving the complex equation $(M_1^{\text{diag}})_{23} = 0$, we find that

$$\tan \phi = \frac{(2b - 3a) \tan \chi}{3a + 2b - 4z \sec \chi} \quad (20)$$

and

$$\tan 2\theta = \frac{2\sqrt{6}z \cos(\chi + \phi)}{3a - 2b \cos 2\phi + 4z \cos(\chi + 2\phi)} \quad (21)$$

for the texture M_1 . Similarly, equating $(M_2^{\text{diag}})_{13} = 0$, we find that

$$\phi = -\chi \quad (22)$$

and

$$\tan 2\theta = \frac{\sqrt{3}z \sin(\phi - \chi)}{2b \sin 2\phi + z \cos \phi \sin(\phi - \chi)} \quad (23)$$

for the texture M_2 . The predictions for the mixing angles θ_{12} and θ_{13} are

$$\sin^2 \theta_{12} = 1 - \frac{4}{\cos 2\theta + 5} \quad \text{and} \quad \sin^2 \theta_{13} = \frac{\sin^2 \theta}{3} \quad (24)$$

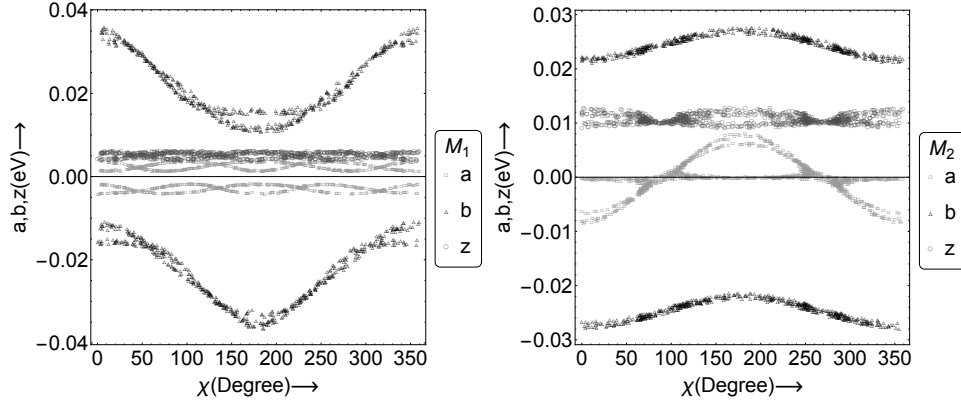


Fig. 1. The allowed parameter space for a, b, z , and χ for the textures M_1 and M_2 .

for the texture M_1 and

$$\sin^2 \theta_{12} = \frac{1}{3 - 2 \sin^2 \theta} \quad \text{and} \quad \sin^2 \theta_{13} = \frac{2 \sin^2 \theta}{3} \quad (25)$$

for the textures M_2 . Here, the variables θ and ϕ are to be substituted from Eqs. (20-21) for the texture M_1 and from Eqs. (22-23) for the texture M_2 .

The diagonal entries of M_1^{diag} are given as

$$(M_1^{\text{diag}})_{11} = 0, \quad (26)$$

$$(M_1^{\text{diag}})_{22} = 3a \cos^2 \theta + 2e^{2i\phi} \sin^2 \theta (b - 2e^{i\chi} z) + \sqrt{6} z \sin 2\theta e^{i(\chi+\phi)}, \quad (27)$$

and

$$(M_1^{\text{diag}})_{33} = 3a \sin^2 \theta + 2e^{2i\phi} \cos^2 \theta (b - 2e^{i\chi} z) - \sqrt{6} z \sin 2\theta e^{i(\chi+\phi)}. \quad (28)$$

Similarly, the diagonal entries for M_2^{diag} are

$$(M_2^{\text{diag}})_{11} = \frac{1}{2} e^{-2i\phi} \left(\sin^2 \theta (4b + e^{i\chi} z) - \sqrt{3} z \sin 2\theta e^{i(\chi+\phi)} - z \cos^2 \theta e^{i(\chi+2\phi)} \right), \quad (29)$$

$$(M_2^{\text{diag}})_{22} = 3a + e^{i\chi} z, \quad (30)$$

and

$$(M_2^{\text{diag}})_{33} = \frac{1}{2} e^{-2i\phi} \left(\cos^2 \theta (4b + e^{i\chi} z) + \sqrt{3} z \sin 2\theta e^{i(\chi+\phi)} - z \sin^2 \theta e^{i(\chi+2\phi)} \right). \quad (31)$$

Substituting the values of θ and ϕ in these entries, we can calculate the three neutrino masses for the textures M_1 and M_2 as

$$m_1 = \left| (M_i^{\text{diag}})_{11} \right|, m_2 = \left| (M_i^{\text{diag}})_{22} \right|, \text{ and } m_3 = \left| (M_i^{\text{diag}})_{33} \right| \quad (32)$$

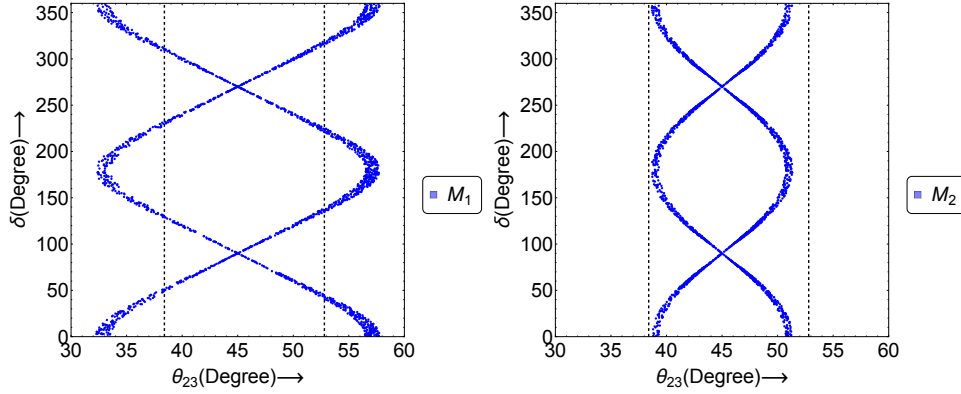


Fig. 2. The correlations between atmospheric angle θ_{23} and CP violating phase δ for both the textures M_1 and M_2 . The two vertical dashed lines enclose the experimentally allowed region of θ_{23} .

for $i = 1, 2$ respectively. We can calculate the mass-squared differences as $\Delta m_{12}^2 = m_2^2 - m_1^2$ and $\Delta m_{23}^2 = m_3^2 - m_2^2$ for both the textures M_1 and M_2 .

We confront these textures with the experimental data²³ by performing a Monte Carlo analysis of the predictions. We generate a set of N random values for each of four free parameters a_j , b_j , z_j , and χ_j with $j = 1, 2, 3, \dots, N$ uniformly in reasonably wide ranges and calculate the predictions for θ_{12} , θ_{23} , Δm_{12}^2 and Δm_{23}^2 using the above relations. We accept only those points (a_j, b_j, z_j, χ_j) for which the calculated values of θ_{12} , θ_{23} , Δm_{12}^2 and Δm_{23}^2 lie in their 3σ experimental ranges²³ depicted in Tab. 1. We depict a , b , and z as functions of χ in Fig. 1. The allowed 3σ ranges of a , b , and z shown in Tab. 2.

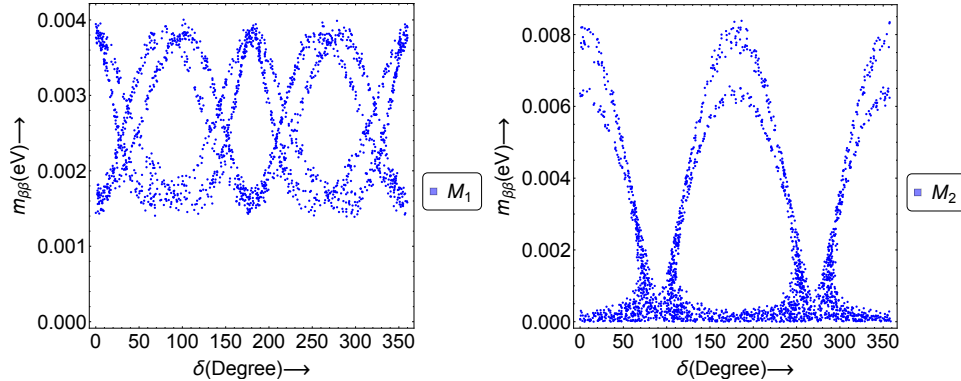


Fig. 3. Variation of $m_{\beta\beta}$ with δ for both the textures M_1 and M_2 .

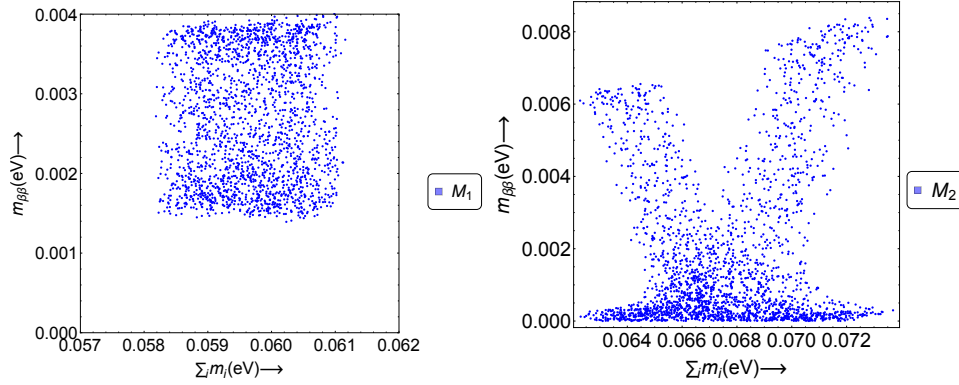


Fig. 4. The allowed region on $(\sum_i m_i - m_{\beta\beta})$ plane for textures M_1 and M_2 .

Table 1. Experimental values of the oscillation parameters.

Parameters	3σ range
$\Delta m_{12}^2/(10^{-5})eV^2$	$7.03 \rightarrow 8.09$
$\Delta m_{23}^2/(10^{-3})eV^2$	$2.407 \rightarrow 2.643$
$\theta_{13}/^\circ$	$7.99 \rightarrow 8.90$
$\theta_{12}/^\circ$	$31.38 \rightarrow 35.99$
$\theta_{23}/^\circ$	$38.4 \rightarrow 52.8$

These textures have testable predictions for θ_{23} and δ . For texture M_1 , we find

$$\sin^2 \theta_{23} = \frac{1}{2} \left(1 + \frac{\sqrt{6} \sin 2\theta \cos \phi}{3 - \sin^2 \theta} \right), \cot^2 \delta = \cot^2 \phi - \frac{6 \sin^2 2\theta \cot^2 \phi}{(3 - \sin^2 \theta)^2}, \quad (33)$$

and for texture M_2 , we find

$$\sin^2 \theta_{23} = \frac{1}{2} \left(1 + \frac{\sqrt{3} \sin 2\theta \cos \phi}{3 - 2 \sin^2 \theta} \right), \csc^2 \delta = \csc^2 \phi - \frac{3 \sin^2 2\theta \cot^2 \phi}{(3 - 2 \sin^2 \theta)^2}, \quad (34)$$

where θ and ϕ are given by Eqs. (20-21) and (22-23), respectively. The correlation plots between θ_{23} and δ has been depicted in Fig. 2. We find that when θ_{23} takes its maximal value of 45° , δ is either 90° or 270° . On the other hand, when θ_{23} takes its extreme values near 40° or 50° , δ is close to either 0° or 180° . We also find that the experimental values of θ_{23} (the region between two vertical dashed lines in Fig. 2) put constraints on δ and it cannot take values around 0 and π for the textures M_1 . The excluded range of δ for the texture M_1 is $[130^\circ, 220^\circ]$ and $[-30^\circ, 30^\circ]$. For the texture M_2 , the whole range of δ is allowed. Such trends can be tested at the experiments like T2K² and NO ν A.¹⁸

The absolute neutrino masses m_1 , m_2 and m_3 can be calculated using relations given in Eq. (32). These masses are not directly observable at the neutrino experiments. The β -decay experiments¹⁹ are sensitive to the effective electron neutrino

Table 2. Allowed ranges of the parameters of mass matrix corresponding to the textures M_1 and M_2 .

Parameters	Allowed 3σ range	
	M_1	M_2
a	$[0.001, 0.004] \cup [-0.004, -0.001]$	$[-0.008, 0.008]$
b	$[0.01, 0.04] \cup [-0.04, -0.01]$	$[0.021, 0.028] \cup [-0.028, -0.021]$
z	$[0.004, 0.006]$	$[0.009, 0.01]$

mass m_β given as

$$m_\beta^2 = m_1^2 |U_{e1}|^2 + m_2^2 |U_{e2}|^2 + m_3^2 |U_{e3}|^2. \quad (35)$$

The neutrino-less double beta decay experiments²⁰ are sensitive to the effective neutrino mass $m_{\beta\beta} = |(M_\nu)_{11}|$ given as

$$m_{\beta\beta} = |m_1 U_{e1}^2 + m_2 U_{e2}^2 + m_3 U_{e3}^2|. \quad (36)$$

The cosmological experiments²¹ are sensitive to the sum of the neutrino masses $\sum_i m_i = m_1 + m_2 + m_3$. We plot $m_{\beta\beta}$ as function of δ in Fig. 3. We depict a correlation between $m_{\beta\beta}$ and $\sum_i m_i$ in Fig. 4. We find that there is a lower bound on $m_{\beta\beta}$ for textures M_1 while there is no lower bound on $m_{\beta\beta}$ for texture M_2 . These predictions will also be testable in the foreseeable future. These textures also have interesting predictions for the Majorana phases α and β :

$$\alpha = \frac{1}{2} \arg \left[\frac{\left(M_i^{\text{diag}} \right)_{22}}{\left(M_i^{\text{diag}} \right)_{11}} \right] \text{ and } \beta = \frac{1}{2} \arg \left[\frac{\left(M_i^{\text{diag}} \right)_{33}}{\left(M_i^{\text{diag}} \right)_{11}} \right] \quad (37)$$

for $i = 1, 2$. We depict the correlation plots for (α, β) and (β, δ) in Fig. 5 for both the textures.

We performed a similar analysis for the textures having inverted hierarchy ($c = a + 2b$ and $d = a + \mu$ in Eqs. (9-10)). We found that we cannot have values of the mixing angle θ_{13} and the ratio $\Delta m_{12}^2 / |\Delta m_{23}^2|$ in their experimental ranges simultaneously. Hence, these textures with inverted hierarchy are ruled out.

In conclusion, we proposed two textures M_1 and M_2 that correspond to the TM_1 and TM_2 mixing schemes respectively and have four free parameters a , b , z , and χ . We show that these textures are consistent with all the current neutrino data. We find the allowed ranges for the parameters a , b , z , and χ and give predictions for θ_{23} , α , β and δ . The predictions for θ_{23} and δ are testable at T2K² and NO ν A.¹⁸

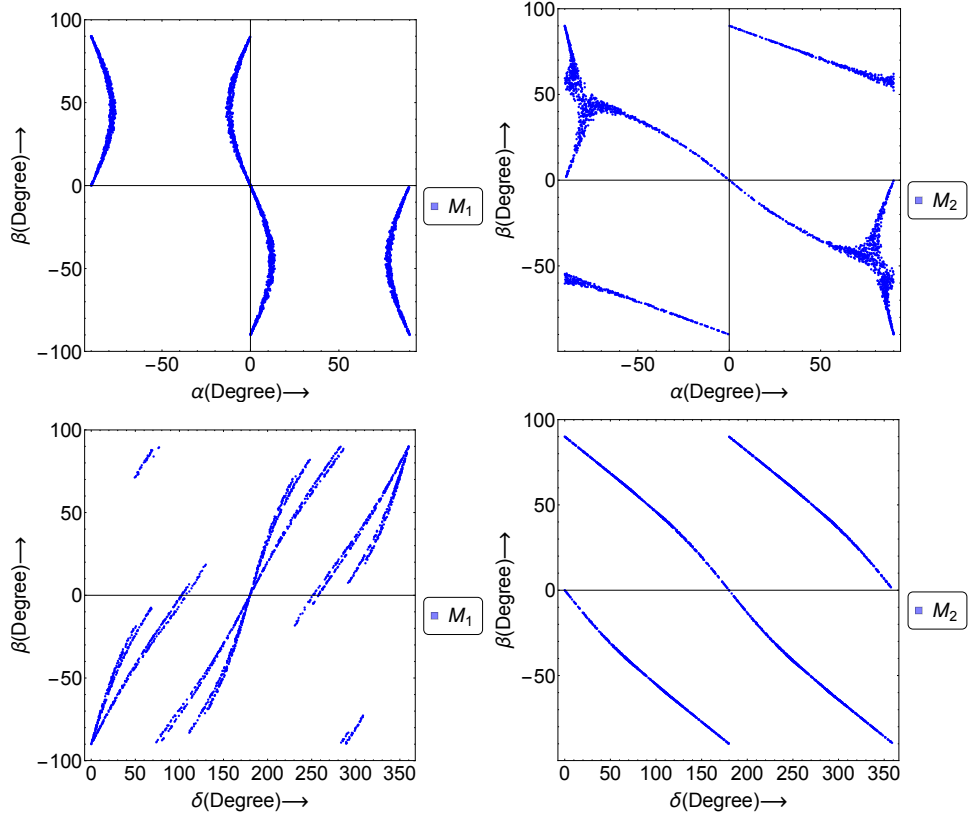


Fig. 5. Correlation plots for Majorana phases α and β for textures M_1 and M_2 .

References

1. K. Olive, *Chin. Phys. C* **38**, 090001 (2014).
2. T2K Collaboration, K. Abe *et al.*, *Phys. Rev. Lett.* **107**, 041801 (2011), [arXiv:1106.2822 \[hep-ex\]](#).
3. Daya Bay Collaboration, F. P. An *et al.*, *Phys. Rev. Lett.* **108**, 171803 (2012), [arXiv:1203.1669 \[hep-ex\]](#).
4. RENO Collaboration, J. K. Ahn *et al.*, *Phys. Rev. Lett.* **108**, 191802 (2012), [arXiv:1204.0626 \[hep-ex\]](#).
5. Double Chooz Collaboration, Y. Abe *et al.*, *Phys. Rev. Lett.* **108**, 131801 (2012), [arXiv:1112.6353 \[hep-ex\]](#).
6. P. F. Harrison, D. H. Perkins and W. G. Scott, *Phys. Lett. B* **530**, 167 (2002), [arXiv:hep-ph/0202074 \[hep-ph\]](#).
7. Z. Z. Xing and S. Zhou, *Phys. Lett. B* **653**, 278 (2007), [arXiv:hep-ph/0607302 \[hep-ph\]](#).
8. C. S. Lam, *Phys. Rev. D* **74**, 113004 (2006), [arXiv:0611017 \[hep-ph\]](#).
9. C. H. Albright and W. Rodejohann, *Eur. Phys. J. C* **62**, 599 (2009), [arXiv:0812.0436](#).
10. C. H. Albright, A. Dueck and W. Rodejohann, *Eur. Phys. J. C* **70**, 1099 (2010), [arXiv:1004.2798](#).
11. X. G. He and A. Zee, *Phys. Rev. D* **84**, 053004 (2011), [arXiv:1106.4359](#).
12. S. Kumar, *Phys. Rev. D* **88**, 016009 (2013), [arXiv:1305.0692](#).
13. P. Harrison and W. Scott, *Phys. Lett. B* **594**, 324 (2004), [arXiv:hep-ph/0403278 \[hep-ph\]](#).
14. R. Friedberg and T. D. Lee, *HEPNP* **30**, 591 (2006), [arXiv:hep-ph/0606071 \[hep-ph\]](#).
15. Z. Z. Xing, H. Zhang and S. Zhou, *Phys. Lett. B* **641**, 189 (2006), [arXiv:hep-ph/0607091 \[hep-ph\]](#).
16. J. D. Bjorken, P. F. Harrison and W. G. Scott, *Phys. Rev. D* **74**, 1 (2006), [arXiv:hep-ph/0511201v2 \[hep-ph\]](#).
17. S. Kumar, *Phys. Rev. D* **82**, 013010 (2010), [arXiv:1007.0808](#).
18. NOvA Collaboration, P. Adamson *et al.*, *Phys. Rev. Lett.* **116**, 151806 (2016), [arXiv:1601.05022 \[hep-ex\]](#).
19. G. Drexlin, V. Hannen, S. Mertens and C. Weinheimer, *Adv. High Energy Phys.* **2013**, 1 (2013), [arXiv:1307.0101](#).
20. W. Rodejohann, *J. Phys. G* **39**, 124008 (2012), [arXiv:1206.2560](#).
21. F. Couchot, S. Henrot-Versillé, O. Perdureau, S. Plaszczynski, B. R. D'Orfeuil, M. Spinelli and M. Tristram (2017), [arXiv:1703.10829](#).
22. C. Jarlskog, *Phys. Rev. Lett.* **55**, 1039 (1985).
23. I. Esteban, M. C. Gonzalez-Garcia, M. Maltoni, I. Martinez-Soler and T. Schwetz, *JHEP* **2017**, 30 (2016), [arXiv:1611.01514](#).